Journal of Physics: Condensed Matter

Magnetic properties of the mixed-valence manganese oxide $Pb_3Mn_7O_{15}$

To cite this article: N V Volkov *et al* 2008 *J. Phys.: Condens. Matter* **20** 055217

J. Phys.: Condens. Matter **20** (2008) 055217 (6pp) doi:10.1088/0953-8984/20/5/055217

Magnetic properties of the mixed-valence manganese oxide $Pb_3Mn_7O_{15}$

N V Volkov[1,2], K A Sablina[1], O A Bayukov[1], E V Eremin[1], G A Petrakovskii[1,2], D A Velikanov[1], A D Balaev[1], A F Bovina[1], P Böni[3] and E Clementyev[4]

[1] Kirensky Institute of Physics SB RAS, 660036 Krasnoyarsk, Russia
[2] Department of Physics, Siberian Federal University, 660041 Krasnoyarsk, Russia
[3] Physics-Department E21, Technical University of Munich, D-85747, Garching, Germany
[4] RFNC-Institute of Technical Physics, 456770 Snezhinsk, Russia

E-mail: volk@iph.krasn.ru

Received 22 June 2007, in final form 19 December 2007
Published 17 January 2008
Online at stacks.iop.org/JPhysCM/20/055217

Abstract

A $Pb_3Mn_7O_{15}$ single crystal has been grown by the flux method and studied using x-ray diffraction and magnetization measurements. The crystal is hexagonal ($P6_3/mcm$ space group, $Z = 4$) and exhibits a pronounced layered nature. Along the [001] direction (c axis), the structure consists of layers of edge-sharing MnO_6 octahedra. Pairs of Mn atoms occupy the octahedral sites located between layers forming 'bridges' along the c axis, which link neighboring Mn layers. The magnetic properties of the crystal have been investigated using ac and dc magnetization measurements in the temperature range 2–900 K at magnetic fields up to 90 kOe. The experimental data obtained suggest that in the temperature region under study several different magnetic phases can be distinguished. Down to ~250 K, the crystal is in the paramagnetic state. Below this temperature, short-range antiferromagnetic ordering apparently starts forming within Mn layers, although a transition to long-range magnetic order occurs at 70 K. The magnetization data obtained leads us to conclude that this state is canted antiferromagnetic with moments lying in the basal plane of the crystal. In addition, below 20 K the crystal undergoes one more magnetic transition that corresponds to spin reorientation.

1. Introduction

Currently, novel materials on the basis of manganese oxides with mixed-valence manganese ions Mn^{3+}/Mn^{4+} are being intensively studied due to their unusual, sometimes intriguing, magnetic and electric properties. These include charge and orbital ordering, a metal/insulator transition, a colossal magnetoresistive (CMR) effect, existence of magnetic phases with competing FM and AFM interactions, and magnetic phase separation. Until recently, attention of researchers has been attracted mainly to doped manganese oxides of the $R_{1-x}E_xMnO_3$ family (R = La, Nd, Pr, Sm, etc, and E = Ca, Sr, Ba, Pb, etc). A perovskite-like structure of these compounds provides high chemical flexibility that allows changing the Mn^{3+}/Mn^{4+} ratio by doping within a wide range with no significant changes of a crystal structure. At the same time, variations of the ratio between Mn ions with different valence in perovskite-like manganites may result in considerable changes of their physical properties. A classical example is the $La_{1-x}Ca_xMnO_3$ system, which graphically demonstrates how strong a level of doping and, consequently, the Mn^{3+}/Mn^{4+} ratio can influence magnetic and electronic states. The (x, H, T)-phase diagram of $La_{1-x}Ca_xMnO_3$ involves ferromagnetic metal, ferromagnetic insulator, canted antiferromagnetic, inhomogeneous magnetic state, charge and orbital ordering states [1–5]. In many respects, richness of the magnetic phase diagram of the crystal is related to coexistence of both antiferromagnetic (AFM) superexchange interactions between Mn^{3+} ions and ferromagnetic (FM) double exchange (DE) interactions between Mn^{3+} and Mn^{4+} ions. The DE interaction results from transfer of an e_g electron between neighboring Mn^{3+} and Mn^{4+} ions through the Mn^{3+}–O–Mn^{4+} path. The specific feature of the DE mechanism is determined by the fact that motion of an itinerant e_g electron favors FM ordering of t_{2g} local spins and, vice versa, the established FM order facilitates motions of itinerant electrons. Thus,

coexistence of Mn ions in different oxidation states is one of the possible reasons for direct correlation between the FM state and conductivity in perovskite-like manganites.

The variety of physical properties (with clear understanding of many phenomena being still lacking) observed in doped perovskite-like manganites excites active search and study of other families of mixed-valence Mn oxides, which do not possess of a perovskite structure. In particular, recently layered manganites of the Ruddlesden–Popper series $(E_{1-y}R_y)_{n+1}Mn_nO_{3n+1}$ and RMn_2O_5 compounds (R is the rare earth ion, either Y or Bi) have been intensively studied. The former includes phases revealing the CMR phenomenon [6], whereas the latter exhibits strong correlation between the magnetic and dielectric properties [7]. We paid attention to the Pb–Mn–O system, which includes a number of phases with compositions suggesting the mixed-valence state of Mn cations. Some compounds belonging to this system were already described [8], yet not thoroughly characterized and studied. Up to date, the available information on the electronic and magnetic properties of the mixed-valence $Pb_3Mn_7O_{15}$ is insufficient. Besides, the results of x-ray study presented by different authors are contradictory. Some authors described the $Pb_3Mn_7O_{15}$ structure in terms of an orthorhombic space group; others indicated that the crystal belongs to the hexagonal space group [9–12]. We should also notice a number of works devoted to characterization of a crystal with the chemical formula referred to as $Pb_3Mn_6O_{13}$ [13]. Similarity of x-ray and magnetic measurement data obtained by different authors suggests that the material under study does belong to the $Pb_3Mn_7O_{15}$ composition. However, the mentioned investigations had rather an incomplete character, so the authors could hardly draw more or less definite conclusion about a crystal structure and magnetic state. Nevertheless, we paid attention to study of the dielectric properties, which suggested arising of the ferroelectric (FE) or anti-FE state. This fact appeared not so surprising, considering the so-called stereoactivity of Pb^{2+} ions [14] that facilitates the creation of local dipoles and, thus, the formation of FE or anti-FE fashion. Possible correlation between the magnetic and dielectric properties has been another reason stimulated the detailed study of $Pb_3Mn_7O_{15}$.

In this paper, we present and discuss the results of thorough investigations of the unique structural and intriguing magnetic properties of the $Pb_3Mn_7O_{15}$ single crystal. Crystallographic structure of the compound has been refined using the single-crystal x-ray diffraction data. Possible magnetic structure has been clarified through analyzing the data of ac/dc magnetization measurements and calculations of Mn–O–Mn interactions made in the framework of an indirect coupling model. We hope that our results and conclusions would be of interest for researchers who study the compounds exhibiting mixed valence of manganese ions and develop models of magnetic interactions in manganese oxides.

2. Experimental details

2.1. Sample preparation

Single crystals were grown by the flux method. As a flux, PbO was chosen, known as an effective solvent for many oxide compounds and allowing to avoid incorporation of foreign ions into a lattice. Synthesis of the $Pb_3Mn_7O_{15}$ crystals started with heating of a mixture of appropriate amounts of high purity PbO and Mn_2O_3 in a platinum crucible at 1000 °C for 4 h. Then the crucible was slowly cooled to 900 °C with a rate $V = 2$–$5\,^{\circ}\mathrm{C\ h^{-1}}$ and, finally, a furnace was cooled to room temperature. The single crystals of a plate–hexagonal form with black shiny surfaces were found at a level of a solidified liquid surface. The plates were up to 40 mm in 'diameter'. The grown crystals were extracted mechanically from the flux. All the measurements reported here were performed on well-polished plate-like samples with a required dimension cut from the resulting single-crystal plates. The samples were oriented by the back-Laue method.

2.2. Experimental measurements

Single-crystal x-ray patterns were collected using a SMART APEX autodiffractometer (Bruker AXS). These data were obtained with a purpose of refining a crystallographic structure at room temperature.

The magnetic properties of the crystal were investigated using ac and dc magnetization measurements performed with a physical property measurement system (PPMS, Quantum Design) in the temperature range from 2 to 350 K at magnetic fields up to 90 kOe. High-temperature (up to 900 K) measurements of magnetic susceptibility were performed with a vibrating sample magnetometer of our original construction.

3. Results

3.1. Crystal structure

Structure of the $Pb_3Mn_7O_{15}$ crystal was refined using the single-crystal x-ray data collected at room temperature. All the reflections were indexed in the hexagonal space group $P6_3/mcm$ with lattice parameters $a = 10.0287(4)$ Å and $c = 13.6137(6)$ Å. The atomic positions, selected bond distances, and bond angles are listed in tables 1–3, respectively. There are four formula units per unit cell. It should be noted that the crystal structure of $Pb_3Mn_7O_{15}$ we found coincides with that of mineral $Pb_3(Fe, Mn)_4Mn_3O_{15}$ known as zenzenite [12], with just minor distinctions in lattice parameters, bonding distances and angles, related apparently to the presence of Fe ions in the mineral.

In figure 1, a crystallographic structure of the compound is schematically presented. Mn cations occupy four crystallographically nonequivalent positions (Mn1, Mn2, Mn3, and Mn4), each of them being coordinated by six oxygen atoms in octahedral configuration. A unit cell includes twelve Mn1 sites (12i) located within slightly compressed oxygen octahedra, eight Mn2 sites (8h) located within trigonal distorted octahedra, two Mn3 sites (2b) coordinated by oxygen atoms in a regular octahedral configuration, and six Mn4 sites (6f) having tetragonal oblate octahedra in environment. Crystallographic structure of $Pb_3Mn_7O_{15}$ has a pronounced layered nature. Along the [001] direction (c axis), the structure consists of layers of edge-sharing MnO_6 octahedra (Mn1, Mn3, and Mn4 positions). Pairs of Mn2 atoms occupy the

Table 1. Structural parameters of $Pb_3Mn_7O_{15}$. For all Pb $U_{iso} = 0.009(1)$ Å^2, for all Mn $U_{iso} = 0.006(1)$ Å^2, for all O $U_{iso} = 0.018(7)$ Å^2. Agreement indices: $R_{wp} = 7.66\%$, $R_p = 9.95\%$.

Atom	Site	x	y	z
Pb1	6g	0.6115(1)	0.6115(1)	3/4
Pb2	6g	0.2652(1)	0.2652(1)	3/4
Mn1	12i	0.8314(1)	0.1685(1)	1/2
Mn2	8h	1/3	2/3	0.147 16(2)
Mn3	2b	0	0	0
Mn4	6f	1/2	1/2	1/2
O1	24l	0.490 63(6)	0.332 20(6)	0.079 66(4)
O2	12j	0.521 3(8)	0.175 2(7)	1/4
O3	12k	0.836 9(8)	0.836 99(6)	0.927 4(5)
O4	12k	0.666 16(8)	0.666 16(6)	0.072 77(5)

Table 2. Selected Mn–O bond lengths for $Pb_3Mn_7O_{15}$ (the left column) and zenzenite [12] (the right column).

Atoms	Bond length (Å) $Pb_3Mn_7O_{15}$	Bond length (Å) zenzenite
Pb1–O1	2.706(8) × 4	2.718(10) × 4
Pb1–O2	2.344(8) × 2	2.301(11) × 2
Pb2–O2	2.275(9) × 3	2.276(10) × 3
Pb2–O4	2.509(10) × 3	2.492(11) × 3
Mn1–O1	1.927(9) × 2	1.904(10) × 2
Mn1–O3	1.982(9) × 2	1.974(12) × 2
Mn1–O4	1.945(8) × 2	1.930(12) × 2
Mn2–O1	1.985(9) × 3	1.974(10) × 3
Mn2–O2	2.070(9) × 3	2.080(11) × 3
Mn3–O3	1.910(8) × 6	1.926(12) × 6
Mn4–O1	1.964(8) × 4	2.002(10) × 4
Mn4–O4	1.939(9) × 2	1.983(11) × 2

Table 3. Selected Mn–O–Mn bond angles for $Pb_3Mn_7O_{15}$.

Atoms	Bond angle (deg)
Mn1–O3–Mn1	95.2(5)
Mn1–O3–Mn3	97.5(5)
Mn1–O1–Mn4	95.4(5) × 2
Mn2–O1–Mn1	126.5(5) × 3
Mn2–O2–Mn2	85.1(5) × 3
Mn2–O1–Mn4	126.1(5) × 3

sites located between the layers that form sort of 'bridges' along the c axis, which link neighboring Mn layers. $Mn2O_6$ octahedra share corners with adjacent manganese octahedra in the layers, and share faces with each other. Lead atoms are located at half a distance between layers and occupy two crystallographically nonequivalent positions, Pb1 and Pb2. They can be described as coordinated by four and six nearest oxygen atoms, respectively, although both Pb1 and Pb2 are off-center in coordination polyhedra.

Local polyhedral distortions observed in $Pb_3Mn_7O_{15}$ may be caused by one of the two following factors. The first corresponds to the possible presence of Jahn–Teller Mn^{3+} ($3d^4$) cations on some Mn sites (a question concerning oxidation states of manganese ions in the crystal will be discussed below). The Jahn–Teller distortions originate from

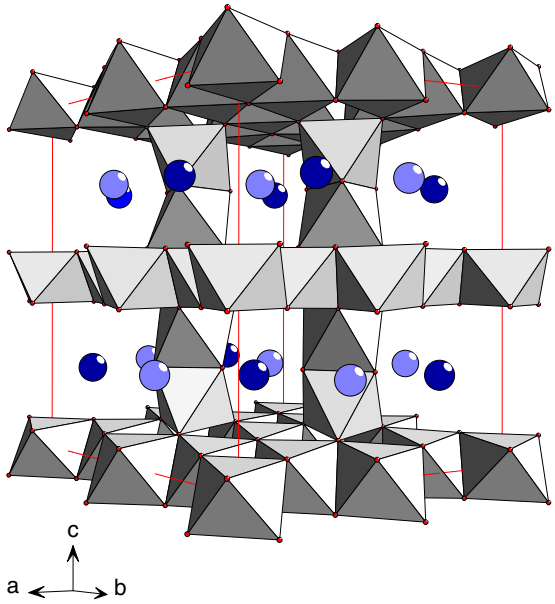

Figure 1. Schematic representation of a crystallographic structure of $Pb_3Mn_7O_{15}$. Mn cations are located in the center of oxygen octahedra; Pb ions are shown as light (Pb1 sites) and dark (Pb2 sites) circles.

(This figure is in colour only in the electronic version)

two degenerate orbital states of a Mn^{3+} ion with electronic configuration $t_{2g}{}^3e_g{}^1$ in the regular octahedral crystal field [15]. The second factor can be associated with stereoactivity of an electron lone pair on $6s^2$ Pb^{2+} ion [14]. Interactions between the lone pair electrons and adjacent bond pairs between cation and ligands give rise to repulsion of the lone pair with the Pb–O bonds. This leads to an asymmetric distribution of the bonds around Pb and, as a result, to significant shifts of some oxygen positions. The assumption that distortions of the coordination octahedra arise due to stereoactivity of Pb^{2+} ions is consistent with a fact that distorted MnO_6 octahedra consist of oxygen ions located in the nearest environment of Pb1 and Pb2 ions. At the same time, the Pb ions occupying both crystallographic sites are not bonded with oxygen atoms of the regular $Mn3O_6$ octahedron.

Now let us consider the question concerning the oxidation states of manganese ions in $Pb_3Mn_7O_{15}$. Authors of all the reports we are familiar [9–12] with suggest that this crystal contains Mn ions in two oxidation states, namely Mn^{3+} and Mn^{4+}, in a ratio 4:3. At the same time, the chemical formula $Pb_3Mn_7O_{15}$ is also consistent with the presence of Mn^{2+} and Mn^{4+} ions in the crystal in a ratio 2:5. Each of the above variants certainly suggests a different magnetic state with own characteristic peculiarities. An analysis of ion sizes for different valence states of Mn and the Mn–O bond lengths make us prefer the variant with the mixed-valence state Mn^{3+}/Mn^{4+}. As for as, valence states and ion sizes are closely related, which allows using a Mn–O bond length to calculate Mn valence via the bond-valence-sum analysis [12]. This method using a tabulated [16] empirical parameters for a cation–anion pairs enables also to extract a reasonable distribution of the trivalent and tetravalent ions

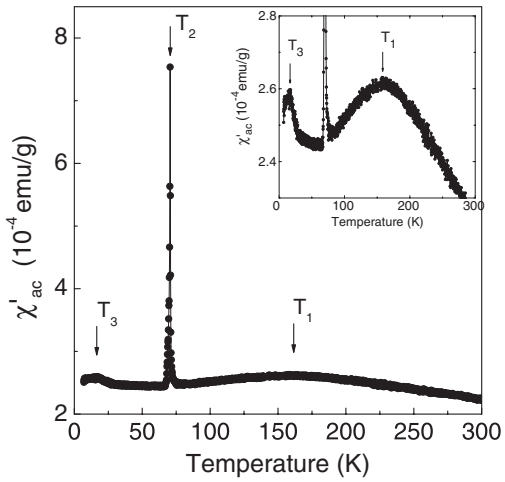

Figure 2. Real part of ac magnetic susceptibility χ'_{ac} as a function of temperature measured at a frequency $f = 1$ kHz and ac field amplitude of 10 Oe without dc bias field. Inset: the same curve in an extended scale.

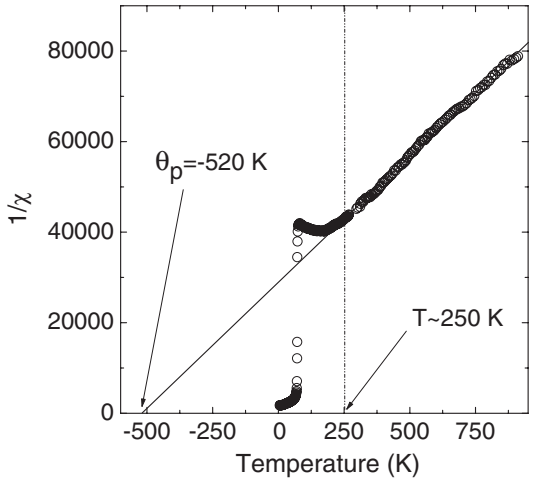

Figure 3. Reciprocal magnetic susceptibility versus temperature ($H = 0.5$ kOe). The solid line is a fit to the Curie–Weiss law.

among nonequivalent Mn sites in the crystal. In our case, the calculated valence for Mn2 and Mn3 are within 0.1 of 3 and 4, respectively, whereas for Mn1 and Mn4 sites the calculation gives intermediate values between 3 and 4. Thus, the bond-valence-sum analysis suggests that the Mn2 site contains only trivalent ions and Mn3 site does only tetravalent ions, whereas the Mn1 and Mn4 sites are occupied by both trivalent and tetravalent ions in common proportion 4:5. In the framework of the model used, it is difficult to make a final conclusion about the distribution of Mn^{3+} and Mn^{4+} among each of the Mn1 and Mn4 sites. To clarify this point, more detailed study is required.

3.2. Magnetic measurements

Figure 2 and the inset their show the temperature dependence of a real part of ac magnetic susceptibility χ'_{ac} for $Pb_3Mn_7O_{15}$ at a frequency $f = 1$ kHz and ac field of 10 Oe without superimposed dc field. A sharp anomaly χ'_{ac} at $T_2 = 70$ K evidently indicates a magnetic phase transition. Two weakly pronounced peaks, which can also be related to the change of a magnetic state, are observed at $T_1 \sim 160$ K and $T_2 \sim 20$ K. In general, ac susceptibilities χ'_{ac} and χ''_{ac} were measured for different frequencies in the range from 10 Hz to 10 kHz for ac field amplitudes from 1 to 10 Oe. Plots of the real χ'_{ac} and imaginary χ''_{ac} parts of susceptibility versus T show no frequency dependence over the measured temperature range, except for the region of low-temperature maximum, where slight dependence of χ'_{ac} and χ''_{ac} versus measuring frequency is observed.

Measurement of dc susceptibility was performed at high temperatures up to 900 K. Figure 3 shows reciprocal susceptibility that has a linear dependence above ~250 K. This indicates that susceptibility follows the Curie–Weiss behavior characterized by a paramagnetic temperature $\theta_p^{exp} = -520$ K and an effective paramagnetic moment $\mu_{eff}^{exp} = 13.3\ \mu_B$ per formula unit. The latter value is close to spin-only values calculated for the mixed-valence state Mn^{3+}/Mn^{4+} of manganese ions in the parent chemical formula $\mu_{eff}^{th} = \sqrt{4(g^2 \cdot 2 \cdot (2+1)) + 3(g^2 \cdot 3/2 \cdot (3/2+1))} \approx 11.9\ \mu_B$ on the assumption that the g-factor equals to 2.

Temperature dependences of dc magnetization M for $Pb_3Mn_7O_{15}$ under the zero-field-cooled and (ZFC) and field-cooled (FC) conditions are given in figure 4. They are presented for two characteristic directions of magnetic field in the crystal: along the sixfold axis ([001] direction) and in the basal plane ([100] direction). Just as in the ac susceptibility measurements, a clear maximum is observed at a temperature $T_1 \sim 160$ K that indicates the onset of the cooperative effect in a magnetic subsystem of the crystal. Generally, the behavior of M in this temperature range is typical for a transition from the paramagnetic to antiferromagnetic state. There are two circumstances, however, worthy of being noted: rather a large width of the maximum and the absence of anisotropy in M below the transition temperature for longitudinal and transverse directions of magnetic field relative to a sixfold axis of the crystal.

Below the temperature $T_2 = 70$ K, where the sharp χ'_{ac} anomaly takes place, M undergoes an abrupt increase for the transverse field direction. Upon further cooling, difference between the FC and ZFC magnetization appears at about 45 K and increases with a decrease in temperature. In ZFC measurements, M reaches a maximal value at 45 K and decreases at lower temperatures; at the same time, in the FC measurements, it increases up to 16 K, remaining practically invariable below this temperature. Such a behavior of M clearly indicates the presence of a weak ferromagnetic effect. Taking into consideration the dependence of M obtained for the longitudinal field direction, we may conclude that the magnetic moment lies in the basal plane of the crystal.

In the region of the low-temperature χ'_{ac} anomaly, M also has peculiarities observed during both the FC and ZFC measurements when a magnetic field direction is in the basal plane. For a longitudinal field direction, these peculiarities become apparent only in high magnetic fields.

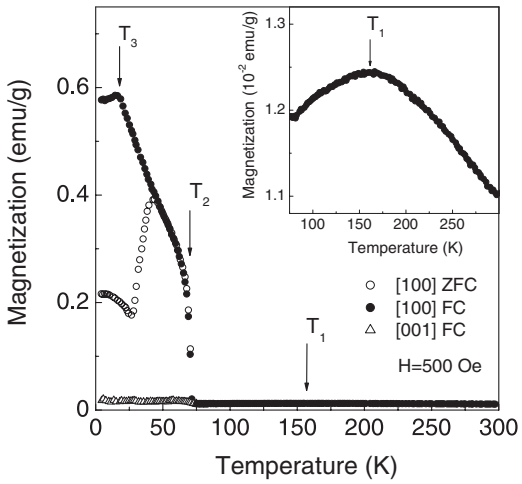

Figure 4. Dc magnetization versus temperature for different directions of magnetic field relative to a crystallographic axis in $Pb_3Mn_7O_{15}$ under the zero-field-cooled (ZFC) and field-cooled (FC) conditions ($H = 0.5$ kOe). Inset: the same curves in an extended scale.

Most likely, the low-temperature anomaly is related to the change of magnetic anisotropic interactions leading to a spin-reorientation transition.

Isothermal magnetization curves for $Pb_3Mn_7O_{15}$ are presented in figure 5. The dependences of M obtained at $H \parallel [100]$ and $H \parallel [001]$ below T_2 confirm the presence of a spontaneous weak ferromagnetic moment lying in the basal plane of the crystal. With a decrease in temperature, the value of spontaneous magnetization increases reaching 0.13 μ_B f.u., which is very small as compared to the theoretical saturation value 25 μ_B (the spin-only one). The magnetization curves for $H \parallel [100]$ show hysteresis for the fields from -20 to 20 kOe at 4.2 K, which abruptly decreases with an increase in temperature and vanishes at T_2. In the case of $H \parallel [001]$, hysteresis phenomena are not observed in the magnetization curves over the measured temperature range.

4. Discussion

The main topic to discuss in this paper is the intriguing magnetic properties of the $Pb_3Mn_7O_{15}$ compound. Crystallographic structure of the compound has a pronounced layer nature that should inevitably cause characteristic peculiarities of the magnetic properties. However, determination of a magnetic structure seems to be fairly a difficult problem to solve because of the obvious complication of $Pb_3Mn_7O_{15}$ structural chemistry. Indeed, although only Mn ions possess of a magnetic moment, the total number of them is 28 per unit cell of the crystal. Besides, they are distributed over the four independent crystal sites, and different sites can be occupied by Mn cations in different oxidation states, which, accordingly, differ in electronic configurations.

Now let us consider a problem concerning magnetic states of $Pb_3Mn_7O_{15}$ realized in different temperature ranges. Approximation of high-temperature susceptibility by the Curie–Weiss law gives unexpectedly high paramagnetic

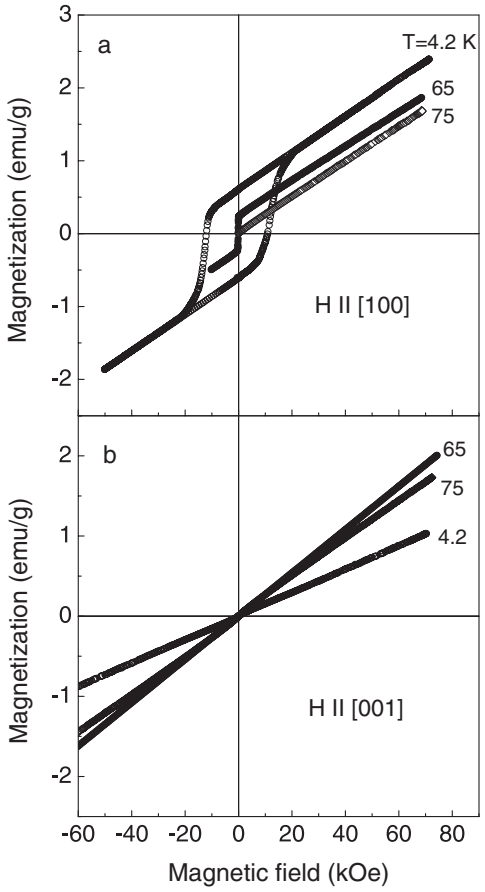

Figure 5. Isothermal magnetization curves for $Pb_3Mn_7O_{15}$: (a) for H in the basal plane ([100] direction); (b) for H along the sixfold axis ([001] direction).

temperature $\theta_p^{exp} = -520$ K, suggesting that interatomic magnetic interactions in the crystal are significant and have an AFM nature over the measured temperature range. The presence of strong exchange interactions is also confirmed by the fact that deviation of magnetic susceptibility from the Curie–Weiss behavior starts at sufficiently high temperatures (∼250 K). Hence, it would be quite reasonable to interpret the maximum in ac and dc magnetizations near 160 K as a transition from the paramagnetic to AFM ordered state. However, this maximum appeared to be too broad for the conventional Néel temperature. This circumstance and, in addition, the absence of anisotropy in the behavior of dc magnetization below the transition temperature expected for the AFM state suggest that the observed specific features of magnetization do not coincide with the onset of long-range magnetic ordering. Possibly, only short-range antiferromagnetic ordering starts forming at this temperature and the clusters may be low-dimensional because of the pronounced layer structure of the crystal. Anyway, at present the origin of the feature in magnetization at 160 K remains a matter of speculation. Magnetization measurements show the onset of the magnetic ordered state in $Pb_3Mn_7O_{15}$ below 70 K. The behavior of magnetization is compatible with a supposition that this state is the canted antiferromagnetic with a weak spontaneous ferromagnetic moment lying in the basal plane of the crystal.

The appearance of hysteresis loops characterized by high coercive fields up to 20 kOe at a temperature of 4.2 K is actually unexpected. It is well known that the high coercivity may arise due to relatively large concentration of defects that hinder motion of magnetic walls or very high magnetocrystalline anisotropy of a sample in the single-domain state. High intrinsic magnetic anisotropy seems fairly a probable reason for the observed high coercivity in $Pb_3Mn_7O_{15}$. Indeed, large magnetocrystalline anisotropy with an easy axis occurring in a uniaxial crystal system ($Pb_3Mn_7O_{15}$ belongs to this type of symmetry) may lead to the high coercivity because the sample cannot become demagnetized without rotating magnetization towards a hard direction. Meanwhile, for the crystal under investigation hysteresis loops are observed only at magnetization lying in the basal plane, although, relative to rotation of the magnetic moments in this plane, magnetic anisotropy should not be high for a hexagonal antiferromagnetic in the easy plane state. Actually, in terms of the thermodynamic approach, the in-plane anisotropy is determined by the sixth order invariants on components of the antiferromagnetism vector.

We can expect arising of domains with noncollinear antiferromagnetism vectors in the basal plane of the crystal, since there are several equivalent antiferromagnetic axes in this plane. When magnetic field is applied along the sixfold axis, domains have equal energies, and the field does not cause a displacement of interdomain walls. In this case, the magnetization process takes place, as if an antiferromagnetic is in the single-domain state. Indeed, the experimental dependences of magnetization do not reveal any peculiarities that would indicate rearrangement of the domain structure. However, when magnetic field is applied in the basal plane, domains are energetically nonequivalent, and the field exerts a pressure on interdomain walls causing their displacement. Irreversible displacement gives rise to magnetic hysteresis. Now we can make no conclusion about the nature of possible anisotropic centers that determine the displacement of interdomain walls, since unambiguous explanation of the observed phenomena certainly requires a detailed micromagnetic study.

5. Conclusion

The $Pb_3Mn_7O_{15}$ single crystal was synthesized; its crystal structure and magnetic properties were investigated. Crystallographic structure of $Pb_3Mn_7O_{15}$ possesses of hexagonal symmetry and has pronounced layered nature. The crystal contains Mn ions in two oxidation states Mn^{3+} and Mn^{4+} in a ratio 4:3. Data of magnetic measurements suggest that several different magnetic phases can be distinguished over the studied temperature region. The paramagnetic behavior is observed at temperatures down to ∼250 K. On further cooling, short-range correlations occur in the system and extensive antiferromagnetic clusters start forming at ∼160 K. At 70 K the long-range magnetic order is established, and low spontaneous magnetization is observed in all the ordered regions. At ∼20 K one more magnetic transition occurs in the crystals, which can be related to reorientation of a magnetic moment.

Acknowledgments

We are grateful to Professor Victor Zinenko (Kirensky Institute of Physics SB RAS) for useful discussion. This study was supported by the INTAS (Project No. 06-1000013-9002) and the Program ‘Spin-dependent Effects in Solids and Spintronics’ of the Division of Physical Sciences of RAS (Project No. 2.4.2 SB RAS). NV also thanks the Foundation for Support of Russian Science.

References

[1] Kim K H, Uehara M, Kiryukhin V and Cheong S W 2004 *Colossal Magnetoresistive Manganites* ed T Chatterji (Dordrecht: Kluwer–Academic)
[2] Rodriguez-Martinez L M and Attfield J P 1996 *Phys. Rev.* B **54** R15622
[3] Dagotto E, Burgy J and Moreo A 2003 *Solid State Commun.* **126** 9
[4] Dagotto E, Hotta T and Moreo A 2001 *Phys. Rep.* **344** 1
[5] Argyriou D N and Ling C D 2004 *Colossal Magnetoresistive Manganites* ed T Chatterji (Dordrecht: Kluwer–Academic)
[6] Chatterji T, Jackeli G and Shannon N 2004 *Colossal Magnetoresistive Manganites* ed T Chatterji (Dordrecht: Kluwer–Academic)
[7] Higashiyama D, Miyasaka S, Kida N, Arima T and Tokura Y 2004 *Phys. Rev.* B **70** 174405
[8] Latourrette B, Devalette M, Guillen F and Fouassier C 1978 *Mater. Res. Bull.* **13** 567
[9] Darriet B, Devalette M and Latourrette B 1978 *Acta Crystallogr.* B **34** 3528
[10] Marsh R E and Herbstein F H 1983 *Acta Crystallogr.* B **39** 280
[11] Le Page Y and Calvert L D 1984 *Acta Crystallogr.* C **40** 1787
[12] Holtstam D, Lindqvist B, Johnsson M and Norrestam R 1991 *Can. Mineral.* **29** 347
[13] Bush A A, Titov A V, Al’shin B I and Venevtsev Yu N 1977 *Russ. J. Inorg. Chem.* **22** 1211
[14] Moore P B, Sen Gupta P K and Le Page Y 1989 *Am. Mineral.* **74** 1186
[15] Levy L P 2000 *Magnetism and Superconductivity* (Berlin: Springer) chapter 2, p 56
[16] Brown I D and Altermatt D 1985 *Acta Crystallogr.* B **41** 244